Inorg. Chem. **2008**, *47*, 6572−6574

Dinuclear Copper(II) Complexes of a Polybenzimidazole Ligand: Their Structures and Inductive Roles in DNA Condensation

Xianggao Meng,[†] Liang Liu,[‡] Chunshan Zhou,[†] Li Wang,[†] and Changlin Liu*[,†]

Key Laboratory of Pesticide & Chemical Biology, Ministry of Education, Central China Normal University, Wuhan 430079, China, and Department of Chemistry, Huazhong University of Science and Technology, Wuhan 430074, China

Received March 24, 2008

The structures of two dinuclear Cu(II) complexes of dtpb were determined. They are shown to be capable of inducing DNA condensation into nanometer- and micrometer-scale particles under neutral conditions.

The dinuclear metal complexes are well-known as artificial metallonucleases and metalloproteases.[1,2] The dinuclear Fe(III), Zn(II), and Cu(II) complexes of a polybenzimidazole ligand, 1,1,4,7,7-pentakis(2′-benzimidazol-2-ylmethyl)triazaheptane (dtpb), have been reported to be capable of cleaving both DNA and proteins via hydrolytic pathways.[3−6] The ligand dtpb is an adaptable and versatile ligand for different transition metal ions because of its flexibility stemming from its aliphatic bridge moiety.

An essential requirement for gene therapy, which utilizes oligonucleotides and plasmid DNA, is the efficient transport of DNA through the cell membrane by processes that are not well-defined.[7,8] Although nonviral DNA delivery vehicles including polyamines, polycationic lipids, and neutral polymers have been shown to be capable of condensing DNA into nanoparticles,[8] the metal complex that can induce DNA condensation has been reported only for the mononuclear complex $[Co(NH_3)_6]^{3+}$.[9−11] Up to now, dinuclear metal complexes have not been reported to be capable of inducing the condensation of DNA.

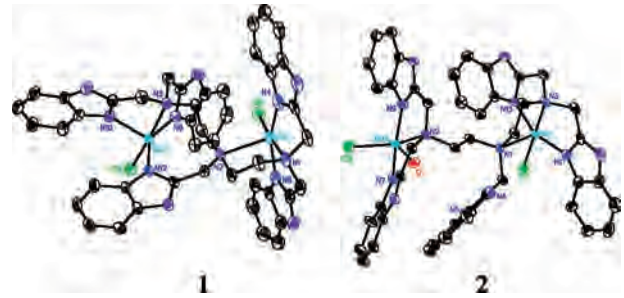

Figure 1. ORTEP view of the dinuclear Cu(II) complexes (**1** and **2**). For clarity, solvent molecules, hydrogen atoms, and counteranions are omitted.

Here, the structures of two dinuclear complexes, $[Cu_2(dtpb)Cl_2]Cl_2$ (**1**) and $[Cu_2(dtpb)Cl_2(H_2O)](NO_3)_2$ (**2**) of dtpb (Figure 1, see Table S1, Supporting Information for cell parameters), and their inductive role in DNA condensation are reported.

In the structure of free dtpb (Figure S1a, Supporting Information; see ref 6 for preparation), five benzimidazole (bzim) groups exhibit a relaxed arrangement. Its dinuclear Cu(II) complexes were prepared by adding a given amount of $CuCl_2 \cdot 2H_2O$ or $Cu(NO_3)_2 \cdot 3H_2O$ into its methanol solutions (see the Supporting Information for preparation and structural determination). The complexes obtained are well-liposoluble, but their solubilities are poor in aqueous solutions.

The dinuclear Cu(II) complexes have a similar overall structure because of the same main ligand, but their coordination geometries of each Cu(II) ion exhibit some subtle differences due to the distinct coordination modes of dtpb and the presence of various auxiliary ligands in the solid state (Figure 1). In **1**, the distorted trigonal-bipyramidal and square-pyramidal geometries around two Cu(II) ions are

* To whom correspondence should be addressed. E-mail: liuchl@mail.ccnu.edu.cn.
† Central China Normal University.
‡ Huazhong University of Science and Technology.

(1) Liu, C.; Wang, M.; Zhang, T.; Sun, H. *Coord. Chem. Rev.* **2004**, *248*, 147–168.
(2) Williams, N. H.; Takasaki, B.; Wall, M.; Chin, J. *Acc. Chem. Res.* **1999**, *32*, 485–493.
(3) Liu, C.; Yu, S.; Li, D.; Liao, Z.; Sun, X.; Xu, H. *Inorg. Chem.* **2002**, *41*, 913–922.
(4) Pan, Q.; Jiang, W.; Liao, Z.; Zhang, T.; Liu, C. *Inorg. Chem.* **2006**, *45*, 490–492.
(5) Yu, S.; Liu, C.; Li, D.; Liao, Z.; Xu, H. *Chin. J. Inorg. Chem.* **2002**, *18*, 1112–1117.
(6) Birker, P. J. M. W. L.; Schierbeek, A. J.; Verschoor, G. C.; Reedijk, J. *J. Chem. Soc. Chem. Commun.* **1981**, 1124–1125.
(7) Luo, D.; Saltzman, W. M. *Nat. Biotechnol.* **2000**, *18*, 33–37.
(8) Vijayanathan, V.; Thomas, T.; Thomas, T. J. *Biochemistry* **2002**, *41*, 14085–14094.
(9) Widom, J.; Baldwin, R. L. *J. Mol. Biol.* **1980**, *144*, 431–453.
(10) Widom, J.; Baldwin, R. L. *Biopolymers* **1983**, *22*, 1595–1620.
(11) Pelta, J.; Livolant, F.; Sikorav, J.-L. *J. Biol. Chem.* **1996**, *271*, 5656–5622.

10.1021/ic800532q CCC: $40.75
Published on Web 07/02/2008

completed by five bzim and three tertiary amine nitrogen atoms of dtpb, and two Cl^- anions. If the weakly axial coordinated N2 atom is considered as nonbonding, the Cu1 coordinated geometry can be described to be a distorted square plane.

Considering the asymmetric distribution of the bzim groups in dtpb and the presence of a remarkable steric effect in **1**, we proposed that the inner coordination spheres of two Cu(II) ions might easily be altered by adding a given equivalent amount of $Cu(NO_3)_2 \cdot 3H_2O$ into the methanol solution of **1**. The results confirmed our hypothesis. Complex **2** was obtained by substituting for one coordinated bzim group to Cu2 with one H_2O molecule. This substitution results in both the appearance of one noncoordinated and relaxed bzim group and the conversion of the coordination geometry around the Cu(II) ion from a trigonal bipyramid in **1** to a square pyramid in **2**. The reasons underlying these significant alterations, which occurred in both the inner and outer spheres of the Cu(II) ions, might be the remarkable steric requirement of coordination and the presence of inter- and intramolecular H bonds mediated by the Cl^- and NO_3^- anions (Figure S2, Supporting Information). The changes that accompany the conversion from **1** to **2** are notable alterations in the bond distances including $Cu-N_{amine}$ and $Cu-N_{bzim}$ bonds and bond angles. For example, the $Cu1-N_{amine}$ bond distances trans to Cl1 are reduced in **2** as compared to those in **1**. Likely, the alterations in the bond distances could be attributed to the significant lattice contributions and the aromatic stacking in the molecular structure. Selected bond lengths and bond angles are listed in Table S2 (Supporting Information) for the complexes.

The extensive $\pi-\pi$ stacking interactions are very similar in these two Cu(II) complexes, although the coordination mode of dtpb in **1** is different from that in **2**. The bzim groups coordinated to Cu1 exhibit a pronounced intermolecular $\pi-\pi$ stacking interaction (Figure S3a, Supporting Information). In the case of **2**, in addition to the $\pi-\pi$ stacking between each pair of coordinated bzim groups, a closely parallel face-to-face $\pi-\pi$ stacking occurs between the imidazole or phenyl rings of the free bzim group in one molecule and the phenyl or imidazole rings of the free bzim group in another adjacent one (Figure S3b, Supporting Information).

In order to understand the role that the dinuclear Cu(II) complexes play in DNA condensation, we first measured the binding equilibrium constant (K_d) of each complex to calf thymus DNA (ctDNA) under neutral conditions (pH 7.4) by UV−visible absorption titration. The data (Figure S4, Supporting Information) showed ~ 1 μM of K_d for each complex, indicating that the affinity of each complex for ctDNA is close to those of DNA intercalators and is not affected by the subtle differences in structure. The similar affinity for ctDNA could be attributed to the ligand exchange occurring easily, which can result in very similar speciation in solution.

The affinity data measured above imply that the intercalation may be one of binding modes of the dinuclear metal complexes to DNA. In order to support this hypothesis, the absorption titration experiments of the complexes with ctDNA were first performed. The data showed that the absorbance of the complexes at 270 nm was gradually reduced with the DNA concentration (Figure S5, Supporting Information), indicating that this hypochromicity is caused by a coupling effect between the π^* orbitals in the complexes and the π orbitals in DNA bases, which is indicative of the intercalation of the ligand in those complexes into the DNA base pairs.[12] Then, the fluorescence dye ethidium bromide (EtBr) that has been confirmed to bind to DNA via an intercalation fashion can serve as a fluorescence probe to explore the binding fashion between each complex and DNA. The data showed that (1) the emission intensity of EtBr bound to ctDNA was reduced over the concentration of each complex (Figure S6, Supporting Information) and (2) the fluorescence intensity of each complex bound to ctDNA decreases upon the addition of EtBr (Figure S7, Supporting Information). These provided an additional support to the binding mode of intercalation for the complexes. In addition, the coordination of DNA bases to the Cu(II) ions should be considered here, since the complexes contain labile ligands H_2O and Cl^-. The electrostatic interactions between each complex and DNA might also not be ignored. Thus, the observed K_d values for the dinuclear Cu(II) complexes might mainly reflect the average of multiple binding fashions.

Then, we examined the role ligand dtpb and its dinuclear Cu(II) complexes played in DNA condensation with light scattering and transmission electron microscopy (TEM) under different conditions. The results showed that both linear λDNA and supercoiled plasmid DNA were condensed immediately into nanoparticles with various profiles and sizes upon the addition of each of the complexes at pH 7.4. The complex doses used here were on the micromolar scale and much less than those of $Co(NH_3)_6^{3+}$ (at least 1 mM) to promote DNA condensation.[11] Moreover, this DNA condensation does not require the addition of Mg^{2+}.[13] The dynamic light scattering (DLS) indicated that the average diameters of DNA nanoparticles in solutions increase first abruptly, then slowly, and finally remain unchanged ($\sim$4000 nm) over the concentration of each complex (Figure 2a) or incubation time (Figure 2b), supported by right-angle light scattering (RALS) measurements (Figure 2c). The pH dependence indicated that the dinuclear metal complex-induced DNA aggregation is most pronounced at pH 7.4, as observed by RALS measurements (Figure 2d). Notable differences were not observed in the DNA condensation between the two complexes. The reasons underlying these results may include the following: (1) the complexes have a similar overall structure; (2) the ligand exchange results in very similar speciation in solution; (3) their interaction fashions with DNA are similar. In addition, inductivity coupled plasma analysis showed the presence of copper with varied amounts in the DNA condensers.

A series of control experiments was performed for comparison. First, the DNA condensation was not found at pH 7.4 but was significantly observed at pH 4.6 for dtpb,

(12) Tysce, S. A.; Baker, A. D.; Strekas, J. C. *J. Phys. Chem.* **1993**, *97*, 1707–1711.
(13) Conwell, C. C.; Hud, N. V. *Biochemistry* **2004**, *43*, 5380–5387.

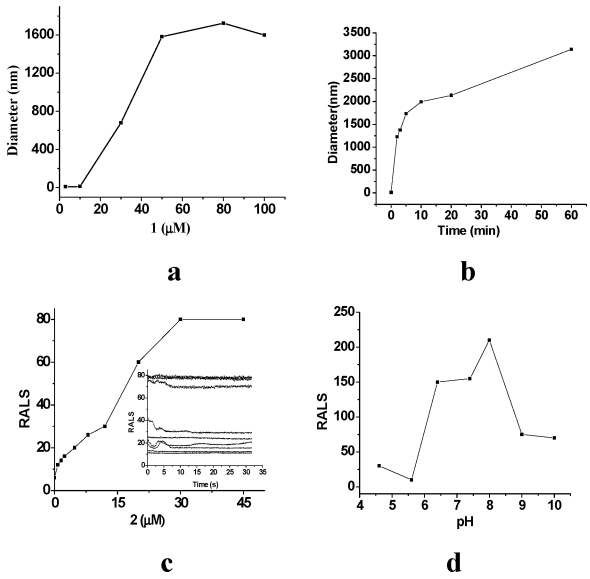

Figure 2. Reaction condition dependencies of DNA condensation. (a) To monitor the complex concentration dependence with DLS, 10 μM λDNA was incubated with **1** (0−100 μM) for 30 min in 20 mM Tris-HCl buffer (pH 7.4) prior to measurement. (b) To monitor the time dependence with DLS, 10 μM λDNA was incubated with **2** (10 μM) for 0−60 min under identical conditions. (c) To monitor the complex concentration dependence with RALS, 10 μM λDNA was incubated with **2** (0−45 μM) for 30 min. Here, the inset shows that the RALS values were changed over incubation time (0−30 min) at each concentration of **2**. (d) To monitor the pH dependence with RALS, 10 μM λDNA was incubated with **1** (10 μM) for 30 min in the buffer solutions of pH 3.5−10. Preparation procedures of the dinuclear Cu(II) complex-induced DNA condensers: The mixtures of λDNA (10 μM in base pairs) and each dinuclear Cu(II) complex at varied doses were incubated for variable periods at room temperature in 20 mM Tris-HCl buffer (pH 7.4) prior to measurement. The resulted DNA condensers were immediately determined by DLS and RALS to evaluate their sizes and were observed under TEM for visualization.

which can be ascribed to its protonation having occurred under acidic conditions that led to multiple positive charges on it. Then, any DNA condensation was not detected with DLS and RALS for both $CuCl_2$ and $Cu(NO_3)_2$ under acidic and neutral conditions. Finally, DNA condensation was also examined for the dinuclear complexes and a mononuclear complex Cu(idb)Cl_2 (see Supporting Information Figure S1b for structure and Figure S4 for binding data with ctDNA, idb, and N,N-bis(2′-benzimidazol-2-ylmethyl)amine, an analogue of dtpb) with RALS under identical conditions, indicating that the RALS values of the condensed DNA induced by the dinuclear complexes is at least 3-fold that by the mononuclear complex. These results indicate that the DNA condensation-driving forces should be both the binding interactions between DNA and each complex and the cooperative effect between two Cu(II) sites. In addition, the intermolecular $\pi-\pi$ interaction of the dinuclear metal complexes might also contribute to DNA condensation.

The profiles of dinuclear Cu(II) complex-induced DNA condensers were examined by TEM. Inspection of the TEM images showed that the dinuclear complexes led first to a collapse of the extended linear or supercoiled DNA into a loose aggregate (Figure 3a) and then further into a compactly globular inclusion with the incubation time at pH 7.4 (Figure 3b). The DNA molecules are arranged in a tree growth ringlike fashion in the inclusions, indicating the formation

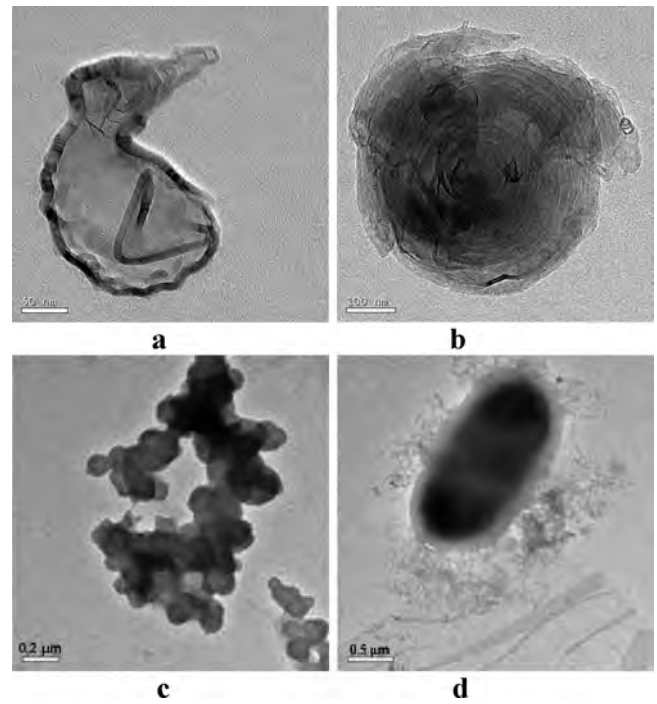

Figure 3. Visualization of DNA condensers under TEM. The DNA nanoparticles were formed by incubation of 5.6 μM λDNA with **2** (10 μM) for 30 (a, b), 60 (c), and 120 min (d) in 20 mM Tris-HCl buffer (pH 7.4).

of the compact inclusions by the entanglement of DNA around a core. The double-stranded DNA is clearly observable here. As the incubation time was prolonged, the nanoparticles could further assemble into an amorphous state (Figure 3c) and a regularly ellipsoid-like structure (Figure 3d) in which the DNA is invisible. These large and dense structures are on the micrometer-scale in size. The DNA dose-dependent DNA condensation was also examined and was similar to the time-dependent process. The condensed DNA is not well-consistent with the reported rodlike and toroidal DNA condensers in morphology and might exhibit a new morphology of DNA condensers. The TEM pictures, together with the size measurements performed in solutions, indicate that DNA is condensed into nanometer- to micrometer-scale particles.

In summary, the structural determination for two dinuclear Cu(II) complexes showed the different ligation modes of dtpb and the presence of labile auxiliary ligands in their coordination spheres. The dinuclear Cu(II) complexes were shown to induce the DNA condensation under neutral conditions. The inductive effect in DNA condensation is observed for the first time for dinuclear metal complexes.

Acknowledgment. This work was supported by NSFC (grand 20571028) and by Key Laboratory of Pesticide & Chemical Biology, Ministry of Education, Central China Normal University (200601A04).

Supporting Information Available: Experimental details, structure determination, Tables S1 and S2, and Figures S1−S7 and X-ray crystallographic files (CIF). This material is available free of charge via the Internet at http://pubs.acs.org.

IC800532Q